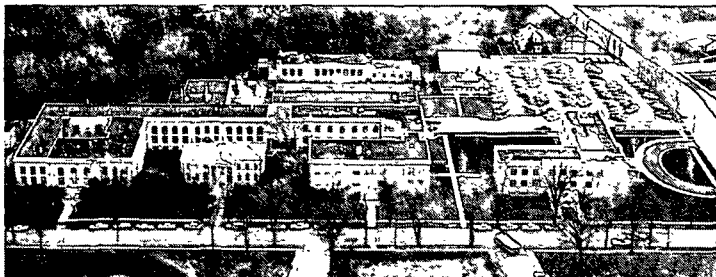


*ms*



THE INSTITUTE OF PAPER CHEMISTRY, APPLETON, WISCONSIN

IPC TECHNICAL PAPER SERIES

NUMBER 195

FUME GENERATION DURING OXIDATION OF ALKALI  
CARBONATE/SULFIDE MELTS

J. H. CAMERON

AUGUST, 1986

## FUME GENERATION DURING OXIDATION OF ALKALI CARBONATE/SULFIDE MELTS

J. H. Cameron  
The Institute of Paper Chemistry  
Appleton, Wisconsin 54912

### ABSTRACT

Air oxidation of  $\text{Na}_2\text{S}$  in  $\text{Na}_2\text{S}/\text{Na}_2\text{CO}_3$  melts produces copious quantities of  $\text{Na}_2\text{CO}_3$  fume. This phenomenon was unexpected and very difficult to interpret in terms of previous concepts of fume production by formation and volatilization of elemental Na or NaOH.

Based on the experimental results obtained in this study, the large quantity of fume which can be generated during sulfide oxidation is a result of Na oxidation in the gas phase. Oxidation of Na in the gas phase significantly lowers the partial pressure of Na. Since the driving force for vaporization is the difference between the equilibrium vapor pressure of Na at the gas-melt interface and the partial pressure of Na in the gas phase, this reduction in partial pressure of Na significantly increases Na vaporization rates and allows fuming to proceed with only mild reducing conditions in the melt.

### INTRODUCTION

One of the principal steps in the kraft pulping process is the recovery of the pulping chemicals. In the recovery process, the black liquor from the pulping process is burned in a recovery furnace. In the furnace, the combustion of the carbonaceous char produced from the pyrolysis of the black liquor occurs in a molten salt environment consisting principally of  $\text{Na}_2\text{CO}_3$  and  $\text{Na}_2\text{S}$ . During the burning of the kraft black liquor a large quantity of fume particles are produced from the volatilization and condensation of the inorganic sodium compounds. These particles are typically 0.25 to 1.0  $\mu\text{m}$  in diameter and are composed principally of  $\text{Na}_2\text{CO}_3$  and  $\text{Na}_2\text{SO}_4$ .

Fume significantly affects the design and operation of the recovery furnace. These particles form deposits on the heat transfer surfaces, reducing heat transfer rates and increasing the amount of surface area required for a given steam load. The fume particles that do not deposit on the heat transfer surfaces are collected by the electrostatic precipitators and recycled into the black liquor. This increases the inorganic content of the black liquor and reduces its heating value on a unit weight basis.

Not all aspects of fume are detrimental. The beneficial aspect of the fume is that it captures the sulfur gases released during black liquor pyrolysis and combustion. This occurs through the reaction of  $\text{Na}_2\text{CO}_3$  with  $\text{SO}_2$  and  $\text{O}_2$  to form  $\text{Na}_2\text{SO}_4$ . This  $\text{Na}_2\text{SO}_4$  is then removed by the precipitators and recycled back into the black liquor.

Recent work by Clay et al. (1984) and Cameron et al. (1985) has shown that air oxidation of  $\text{Na}_2\text{S}$  in a  $\text{Na}_2\text{S}/\text{Na}_2\text{CO}_3$  melt can produce large quantities of  $\text{Na}_2\text{CO}_3$  fume. The rate of fume generation under oxidizing conditions was found to be considerably greater than the rate under strongly reducing conditions. This phenomenon was unexpected and very difficult to interpret in terms of the existing concept of fume formation by elemental Na formation and volatilization at high-temperature reducing conditions. This paper describes the mechanism responsible for fume generation during air oxidation of  $\text{Na}_2\text{S}$  in a  $\text{Na}_2\text{S}/\text{Na}_2\text{CO}_3$  melt.

#### PREVIOUS WORK

Several researchers have used thermodynamic equilibrium calculations to predict the liquid and gaseous species present in the kraft furnace. Bauer and Dorland

(1964) were one of the first to apply this technique to the kraft furnace. Their study predicted that the volatile fuming species in the furnace are Na and Na<sub>2</sub>. They considered NaOH as a liquid species but not as a gaseous species. Thus they a priori eliminated it as a potential source of fume.

More recently Warnqvist (1973) also applied equilibrium thermodynamics to the kraft furnace and concluded that in addition to Na and Na<sub>2</sub>, NaOH is an important volatile compound. Warnqvist believed that the earlier study by Bauer and Dorland (1954) was flawed for not including NaOH(g) in the equilibrium calculations.

As stated by Warnqvist (1973) a major assumption in these equilibrium treatments is that "the waste liquor/air (oxygen) system as a whole comes to chemical equilibrium." This assumption is recognized to be somewhat unrealistic, but Warnqvist believed that this technique provides an insight into the processes and chemical species present in the furnace.

Equilibrium treatments predict that the major fume producing species are Na, Na<sub>2</sub>, and NaOH. The vaporization rate of a chemical species can be significantly affected by the reaction between the volatile species and any gaseous species, as indicated by Turkdogan (1963). Since furnace gases such as O<sub>2</sub> and CO<sub>2</sub> are reactive with Na and Na<sub>2</sub>, equilibrium treatments cannot be used to predict the amount of fume generated through Na and Na<sub>2</sub> vaporization. They can, however, be used to predict the melt composition and the vaporization rate of nonreactive species such as KCl, NaCl, and possibly NaOH.

Turkdogan (1980) states that there are two possible mechanisms for enhanced vaporization of a liquid into a reactive gas: (1) the gas may react with the liquid to form a volatile species or (2) the gas may react with the

vapor from the liquid, lowering the partial pressure of the vapor above the liquid and enhancing the vaporization rate.

Turkdogan et al. (1963, 1980, 1982) have shown that the oxidation of many molten metals can produce large amounts of metal oxide fume. Since there are several similarities between these fuming systems and fuming during sulfide oxidation in a carbonate melt, a review of fuming during oxidation of molten metals is included here.

The increase in fuming during oxidation in these molten metals is attributed to the reaction of the metal vapor with oxygen to form a condensed metal oxide fume. This may be considered to be a counterflux transport process. Oxygen diffuses toward the molten metal surface, and metal vapor diffuses away from the surface. At some distance from the surface the metal vapor and oxygen react to form a metal oxide condensed phase (Figure 1).

(Figure 1 here)

This reaction in the gas phase forms a sink for the metal vapor, reducing its partial pressure. Since the driving force for vaporization is the difference between the vapor pressure of the metal and its partial pressure in the gas phase, this reduction in partial pressure can greatly enhance the rate of vaporization.

The maximum rate of the metal vaporization with this mechanism is equal to the vaporization rate in a vacuum. At the maximum vaporization rate, the metal oxide fume is forming directly at the metal surface. If the oxygen partial pressure is increased beyond this value, the flux of oxygen toward the metal surface is greater than the vaporization rate of the metal. Oxidation

then occurs within the molten metal, forming a metal oxide film. Since the concentration of the volatile species is greatly reduced in this metal oxide film, the formation of this film results in a significant decrease in the vaporization rate of the metal.

#### EXPERIMENTAL APPARATUS

The fume generation experiments were conducted by monitoring the fume produced from alkali carbonate/sulfate/sulfide melts under different atmospheres. The experimental system consisting of an induction heated reactor, gas meters and fume filter is illustrated in Figure 2. The ceramic reactor was normally charged with approximately 85 g of inorganic salts containing 53 to 80 g of  $\text{Na}_2\text{CO}_3$ , 2.0 to 20 g of  $\text{Na}_2\text{S}$ , and 0 to 40 g of  $\text{Na}_2\text{SO}_4$ .

(Figure 2 here)

Two configurations for introducing the purge into the reactor were employed during this study. These configurations consisted of either introducing the  $\text{N}_2/\text{O}_2$  gas mixture directly into the melt or into the reactor above the melt. Figure 2 illustrates the experimental system with the gases introduced below the melt's surface. With the gases introduced into the melt, oxygen was totally consumed by sulfide oxidation. With the gases introduced above the melt, the sulfide content of the melt was oxidized without any significant mixing of the melt. This configuration would tend to produce a melt with an oxidized surface and also resulted in a residual  $\text{O}_2$  concentration above the melt. The effect of residual  $\text{O}_2$  was studied by adding different amounts of  $\text{O}_2$  to the carrier gas.

The fume generation rate was followed by filtering the off-gas and weighing the fume particles. To ensure that this gravimetric method collected

all the fume particles, the Na content of the off-gas after the filter was checked with a flame photometer. Readings from the flame photometer showed that the filter collected essentially all the fume particles.

The fume particles collected during sulfide oxidation were typically white spherical particles approximately 0.25 to 1.0  $\mu\text{m}$  in diameter. Figure 3 is a scanning electron micrograph (SEM) of fume particles collected during sulfide oxidation. Infrared analysis of these fume particles revealed that they are essentially pure  $\text{Na}_2\text{CO}_3$ .

(Figure 3 here)

#### FUME GENERATION WITH GAS INTRODUCED BELOW THE MELT'S SURFACE

In this section, the effects of sulfide concentration, sulfate concentration, temperature, inlet oxygen content, and gas flow rate on fume generation with the gas introduced directly into the melt are described.

##### Typical Experimental Results with Gas Introduced Below the Melt's Surface

In a typical experiment, the fume generation rate was monitored by filtering the off-gas from the reactor for a five-minute period and weighing the fume collected. Experimental results typical of the majority of the experiments conducted using this procedure are illustrated in Table 1.

(Table 1 here)

It can be seen that the fume generation rate remains at a constant level until the sulfide is nearly totally oxidized. Once the sulfide level reaches a concentration of approximately 0.1 mole/L, the fume generation rate rapidly decreases. Although the relative concentrations of sulfide and sulfate

change significantly during this experiment, little change in the fume generation rate is observed until the sulfide is nearly completely oxidized. This indicates that the ratio of sulfide to sulfate has little effect on the fume generation rate.

#### Effect of Sulfate Concentration

To determine the effect of sulfate concentration on the rate of fume generation, the fume generation rate was measured at two different initial amounts of sulfate in the melt. The rate of fume generation was followed using the previously described gravimetric method. The results of these experiments are presented in Table 2.

(Table 2 here)

It can be seen that sulfate concentration in the melt does not significantly affect the fume generation rate. Although the melt in Run 43 contained a high level of sulfate, the fume generation rate was only slightly different from that in Run 39 with no initial sulfate present.

#### Effect of Sulfide Concentration

To determine the effect of sulfide concentration on the rate of fume generation, the fume generation rate was measured with different initial amounts of sulfide in the melt. The effect of sulfide on the rate of fume generation is shown in Table 3.

(Table 3 here)

It is obvious that the amount of sulfide has no significant effect on the rate of fume generation.

### Effect of Oxygen Partial Pressure on Fume Generation Rate

To determine the effect of inlet oxygen concentration on the rate of fume generation, the oxygen level in the purge was varied. Preliminary studies of sulfide oxidation with O<sub>2</sub>/N<sub>2</sub> mixtures introduced below the melt's surface have shown that essentially all the oxygen supplied to the melt is consumed by sulfide oxidation. Therefore, to maintain a constant off-gas flow rate from the melt, the nitrogen flow to the reactor was held constant and the oxygen flow was adjusted. The results of a series of experiments with varying inlet oxygen concentrations are shown in Table 4.

(Table 4 here)

As shown in this table, the increase in oxygen to the reactor tends to increase the rate of fume generation. However, the fume dependence on the oxygen concentration rate is slight. Although the initial concentration of oxygen in Table 4 increased by a factor of eight, the fume rate less than doubled.

### Temperature Effect

To determine the temperature dependence, fume generation rates were measured during Na<sub>2</sub>S oxidation at temperatures ranging from 927 to 1038°C. By plotting the ln of the fume generation rate vs. 1/T, °K<sup>-1</sup> it was found that the fume generation had an Arrhenius type temperature dependence with an activation energy of approximately 20,000 cal/mol, as shown in Figure 4.

(Figure 4 here)

### Effect of Nitrogen Flow Rate on Fume Generation

To determine the effect of the volumetric flow rate on the fume generation rate, the nitrogen flow rate was varied while the oxygen flow rate was

held constant. Since the oxidation rate is limited by the amount of oxygen supplied, the oxidation rate remained the same for each experiment. The results of these experiments using the gravimetric method of following fume generation are given in Table 5.

(Table 5 here)

It is evident that the fume generation rate is nearly proportional to the volumetric purge rate.

#### Surface Area Effect

The objective of these experiments was to determine if a change in the surface area of the bubbles would affect the fume generation rate. To increase the melt-gas interface, the single purge tube (0.475-cm ID) was replaced with two purge tubes (0.158-cm ID).

The fume generation rates from several sulfide oxidation experiments employing the two purge tubes are shown in Table 6. Also shown in this table are the fume generation rates for the single purge tube.

(Table 6 here)

It can be seen that the fume generation rate using the two purge tube system is nearly the same as that for the single purge tube. Therefore, changes in the melt-gas interfacial area have little effect on the fume generation rate.

#### Effect of Different Inert Carrier Gases

To determine the effect of gas phase processes, fume generation was studied using different carrier gases. The carrier gas is the inert gas with which the oxygen is mixed. If the rate controlling process for fume generation

during sulfide oxidation is a liquid phase process, the type of carrier gas used should not affect the rate of fume generation. However, if the rate controlling process is a gas phase process, the fume generation rate could be dependent on the type of carrier gas used. Fume generation rates using three different carrier gases are shown in Table 7.

(Table 7 here)

With He as the carrier gas, the fume generation rate was significantly lower than the fume generation rates observed with either N<sub>2</sub> or Ar as carrier gas. This indicates that gas phase processes are significant in fume generation during sulfide oxidation.

#### FUMING WITH OXYGEN-NITROGEN GAS INTRODUCED ABOVE MELT'S SURFACE

To determine the effect of the mode of gas-liquid contact on oxidative fuming, fume generation during sulfide oxidation was studied with the purge tube located above the melt. Typical fume generation rates during sulfide oxidation using this mode of gas-melt contact are illustrated in Figure 5 and 6.

Figure 5 illustrates the fume generation rates for low levels of oxygen in the purge. At these rates of oxidation, there is not much change in the melt composition, and the rate of fume generation remains essentially constant. Figure 6 illustrates the fume generation rates for higher levels of oxygen in the purge. At these rates of oxidation, the rate of fume generation decreases as the sulfide content of the melt is oxidized to sulfate.

(Figure 5 and 6 here)

These figures show that the oxidation of a sulfide in a sulfide-carbonate melt with the oxygen introduced above the melt usually results in a decrease in the fume generation rates compared to that observed under a pure N<sub>2</sub> purge. Only at extremely low levels of oxygen did the fume generation rate increase. This is in distinct contrast to the large level of fume observed when the gas was introduced into the melt.

In Table 8, the fume generation rates during sulfide oxidation with the purge introduced above the melt's surface are compared to the rates with the purge introduced below the melt's surface. Since the fume generation rate fell off with time during sulfide oxidation when the purge was introduced above the melt's surface, the fume generation rates in Table 8 for this configuration are the initial rates. At the same sulfide oxidation rate, the fume generation rates with the purge introduced above the melt's surface are approximately an order of magnitude lower than those with the purge introduced below the melt's surface.

(Table 8 here)

Equal rates of sulfide oxidation can be achieved with both modes of gas-melt contact. Therefore, if fume results from the formation of a volatile species during sulfide oxidation, this species should be formed in both modes of gas-melt contact. Since little fume is generated when the gas is introduced above the melt's surface, it is unlikely that fume generation during sulfide oxidation results from the formation of a new volatile compound.

The second critical experiment in the development of the fume generation mechanism is the effect of the inert carrier gas on fume generation. The fuming rate with He as the carrier gas was significantly lower than that with either N<sub>2</sub> or Ar as the carrier gas. This indicates that fume formation is a

gas-phase controlled process. It is also a further indication that fume is not the result of the formation of new volatile compounds. The formation of such compounds would be controlled by liquid-phase processes, and the fume generation rate would then be independent of the type of carrier gas used.

#### Mechanism for Fume Generation under Oxidizing Conditions

Based on the experimental results obtained in this study, the following theory is proposed to explain fume generation during sulfide oxidation:

The enhancement of fume generation observed during sulfide oxidation results from the oxidation of Na in the gas phase.

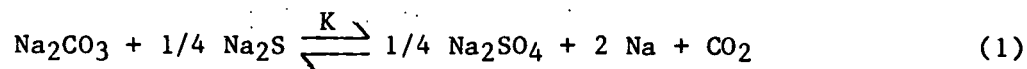
This oxidation greatly lowers the partial pressure of Na in the gas phase, increasing Na vaporization from the melt.

Sodium sulfide in the melt is a sufficiently strong reducing agent to produce a significant Na partial pressure. The liquid and gas phase processes occurring during oxidation-enhanced fume generation are illustrated in Figure 7. Sodium and CO<sub>2</sub> are generated in the melt from the equilibrium reaction between Na<sub>2</sub>CO<sub>3</sub> and Na<sub>2</sub>S, as given by Eq. (1). The Na and CO<sub>2</sub> then evaporate and react with O<sub>2</sub> diffusing toward the melt at some distance  $\delta$  from the melt. A detailed description of this fume generation mechanism is presented below.

(Figure 7 here)

#### Liquid Phase Processes

The processes responsible for fume generation during sulfide oxidation can be separated into those processes occurring in the liquid phase and those occurring in the gas phase. In the liquid phase, the concentration of Na in the melt is assumed to be dependent on the equilibrium given by Eq. (1).



Since the melt used for this study consisted primarily of  $\text{Na}_2\text{CO}_3$ , the activity of  $\text{Na}_2\text{CO}_3$  is assumed to be approximately 1.0. Then assuming ideal behavior for the  $\text{Na}_2\text{S}$  and  $\text{Na}_2\text{SO}_4$ , the partial pressure for sodium is described by Eq. (2).

$$P_{\text{Na}} = \frac{K^{1/2} [X_{\text{Na}_2\text{S}}]^{1/8}}{[X_{\text{Na}_2\text{SO}_4}]^{1/8} [P_{\text{CO}_2}]^{1/2}} \quad (2)$$

Here,  $P_M$  is the partial pressure of component M;  $X_M$  is the mole fraction of component M; and K is a constant.

Equation (2) indicates that the equilibrium vapor pressure of Na is only very weakly dependent on the  $\text{Na}_2\text{SO}_4$  and  $\text{Na}_2\text{S}$  concentrations in the melt. This explains why changes in the  $\text{Na}_2\text{SO}_4$  and  $\text{Na}_2\text{S}$  concentrations have little effect on the fume generation rate until only a very low concentration of  $\text{Na}_2\text{S}$  remains in the melt.

#### Gas Phase Processes

The most significant process occurring in the gas phase is the oxidation of Na, which lowers the partial pressure of Na in the gas. Since the rate of Na vaporization depends on the difference between the vapor pressure of Na at the melt-gas interface and the partial pressure in the gas, the reduction in partial pressure increases the Na vaporization rate.

The reactions occurring in the gas phase are represented by Eq. (3) and Eq. (4).



These equations are not intended to represent a mechanism, but are intended to indicate the stoichiometry of the gas phase reactions.

The consumption of  $\text{CO}_2$  in the gas also increases the rate of Na vaporization. If only Na was consumed in the gas phase reactions, the  $\text{CO}_2$  generated would shift the equilibrium represented by Eq. (1) toward the left and result in a lower vapor pressure for Na.

#### APPLICATION OF FUME GENERATION THEORY TO THE EXPERIMENTAL RESULTS

Described below is the application of the proposed fume generation theory to the two modes of gas-melt contact used during this study. In one mode of gas-melt contact, the  $\text{O}_2\text{-N}_2$  stream was introduced above a relatively quiescent melt. With this mode of oxidation, little fume was observed and the rate of fume generation decreased as the  $\text{O}_2$  partial pressure was increased.

In the other mode of gas-melt contact, the  $\text{O}_2\text{-N}_2$  stream was introduced below the melt's surface. This mode of oxidation generated a high level of fume. Although the fume generation rate was not highly dependent on the  $\text{O}_2$  content of the purge, the fume generation rate increased as the  $\text{O}_2$  content of the gas increased.

#### Interpretation of Fume Generation with Gas Introduced above Melt's Surface

The fume generation behavior observed with the gas introduced above the melt is very similar to that reported in Turkdogan's (1963) study of fuming

during the oxidation of molten metals. At low  $O_2$  partial pressure, the Na evolving from the melt is oxidized above the melt, lowering the partial pressure of Na and increasing the rate of Na vaporization. At higher  $O_2$  partial pressures, the  $O_2$  penetrates to the melt surface. Oxidation of the Na and  $Na_2S$  then occurs in the melt and little fume is generated.

The vapor pressure of Na above a  $Na_2S-Na_2CO_3$  melt is relatively low compared to the vapor pressure of the metal systems studied by Turkdogan (1963, 1980, 1982). The  $O_2$  partial pressure required to penetrate the boundary layer to the melt surface is also relatively low for Na in the  $Na_2S-Na_2CO_3$  melts compared to the metal systems. Therefore, with the gas introduced above the melt, an increase in fume generation is observed only at low  $O_2$  partial pressures. While in the metal systems, an increase in fume generation occurs even at relatively high  $O_2$  partial pressures.

#### Interpretation of Fume Generation with Gas Introduced below Melt's Surface

The fuming behavior during sulfide oxidation with the gas introduced below the melt's surface was considerably different than that observed with the gas introduced above the melt. The major difference was the relatively high level of fuming during  $Na_2S$  oxidation. The effect of  $O_2$  partial pressure was also significantly different in the two modes of gas-melt contact. With the gas stream introduced below the melt's surface, increasing the  $O_2$  partial pressure in the purge resulted in a slight increase in the rate of fume generation. This contrasts to the decrease in fume generation with an increase in  $O_2$  partial pressure when the gas was introduced above the melt. The  $Na_2S$  concentration in the melt had different effects on the rate of fuming in the two modes of melt-gas contact. With the gas introduced above the melt, fuming rate

decreased as the  $\text{Na}_2\text{S}$  was oxidized to  $\text{Na}_2\text{SO}_4$ . With the gas introduced below the melt's surface, the level of  $\text{Na}_2\text{S}$  concentration had no effect on the fuming rate until only low levels of  $\text{Na}_2\text{S}$  remained in the melt.

With the gas introduced below the melt's surface, fume is generated in the bubble as it rises in the melt (Figure 8). The liquid surrounding the bubble is continually renewed, and as a result of the liquid flowing past the bubble the gas in the bubble may undergo toroidal circulation. The basic difference between this mode of oxidation and oxidation with the gas introduced above the melt is the mixing of the liquid at the gas-melt interface.

(Figure 8 here)

In a gas-liquid reaction, the reaction rate may be limited by (A) gas side mass transfer, (B) liquid side mass transfer, (C) the chemical kinetics, or (D) a combination of these processes. Since the oxidation of  $\text{Na}_2\text{S}$  in a carbonate melt is an extremely fast reaction and preliminary experiments showed that it is independent of  $\text{Na}_2\text{S}$  concentration, it is probable that this reaction is mass transfer limited. When the purge tube was located above the melt's surface, only low levels of fume were observed during sulfide oxidation. In this mode of oxidation, the reaction is limited by liquid side mass transfer.

Since large amounts of fume were generated during sulfide oxidation when the gas was introduced below the melt's surface, the melt at the liquid-gas interface is unoxidized in this mode of sulfide oxidation. The sulfide oxidation reaction is then limited by either gas side mass transfer or by chemical kinetics. If kinetics limits the oxidation rate, the majority of the chemical species in the melt at the interface should be oxidized and the fraction of oxidized species should be dependent on the  $\text{O}_2$  partial pressure in the purge gas.

This situation would be similar to that with the purge tube introduced above the melt. The fume generation rate should be low and should decrease as the  $O_2$  partial pressure in the gas is increased. Since a high level of fume was present and the fuming rate increases with an increase in  $O_2$  partial pressure, the oxidation rate is not kinetically limited, but is likely gas-phase mass transfer limited.

The effect of different carrier gases on the fume generation rate, shown in Table 7, also indicates that the sulfide oxidation rate is not limited by the chemical kinetics. Helium, the carrier gas in which the diffusivities are the highest, produced the lowest fuming rate. If the  $Na_2S$  oxidation reaction was limited by the chemical kinetics, the carrier gas would not affect the reaction rate. The vapor pressure of the volatile species would not be affected by the carrier gas and the only effect the carrier gas would have would be on the rate of flux of the volatile species from the surface. Carrier gases with higher diffusivities such as He would have higher fluxes of the volatile species and would produce higher fuming rates. Since He produced the lowest fuming rate, the reaction rate and fume generation process are not limited by the chemical kinetics.

As the gas bubble rises in the melt, the melt at the interface is constantly mixed. This mixing of the melt and the fast rate of the oxidation reaction results in the reaction being controlled by gas-side mass transfer. Figure 9 illustrates the relative  $O_2$ , Na, and  $Na_2S$  concentrations at the interface during  $Na_2S$  oxidation.

(Figure 9 here)

The  $O_2$  partial pressure in the gas falls to near zero at the interface. Since the melt is renewed at the interface faster than it is oxidized, the Na and  $Na_2S$  concentrations at the interface are nearly identical to those in the bulk melt.

In this situation, Na evolves from the melt and is oxidized near the interface in the gas. This oxidation lowers the partial pressure of Na in the gas and significantly enhances the rate of Na evolution. Since the melt at the interface is constantly renewed, its composition remains constant as the  $O_2$  in the bubble is consumed. The fume generation rate is constant as long as sufficient  $O_2$  remains in the gas to rapidly oxidize the Na evolving from the melt. The fume generation rate observed then depends on the time required for consumption of the  $O_2$  in the bubble.

The rate of  $O_2$  consumption is described by Eq. (5).

$$\frac{d(N_{O_2})}{dt} = S K_g (P_{O_2} - P_{O_2}^*) \quad (5)$$

Here,  $P_{O_2}$  is the partial pressure of  $O_2$  in the bulk gas;  $P_{O_2}^*$  is the partial pressure at the interface;  $K_g$  is the gas phase mass transfer coefficient;  $N_{O_2}$  is moles of  $O_2$ ; and  $S$  is interfacial surface area.

Since  $P_{O_2} \gg P_{O_2}^*$ , Eq. (5) can be written as:

$$\frac{d(N_{O_2})}{dt} = S K_g P_{O_2} \quad (6)$$

The partial pressure of  $O_2$  in the gas is shown in Eq. (7):

$$P_{O_2} = \frac{N_{O_2}}{N_{N_2} + N_{O_2}} \times P_t \quad (7)$$

Here,  $P_t$  is the total pressure, and  $N_{N_2}$  is moles of  $N_2$ .

For the experimental conditions used in this study the  $O_2$  content in the gas during sulfide oxidation is much less than the  $N_2$  content of the gas. The partial pressure of  $O_2$  is then approximated by Eq. (8).

$$P_{O_2} = \frac{N_{O_2}}{N_{N_2}} Pt \quad (8)$$

The rate of  $O_2$  consumption is then given by Eq. (9)

$$\frac{d(N_{O_2})}{dt} = S Pt K_g \frac{N_{O_2}}{N_{N_2}} \quad (9)$$

During sulfide oxidation, the fume generation rate remains constant until the  $O_2$  level in the gas bubble falls below that required to rapidly oxidize the Na being evolved. The weight loss of the melt due to fuming (or fume generated during this period) is then described by Eq. (10).

$$\frac{dF}{dt} = - S K \quad (10)$$

Here,  $F$  is the weight of material evolved from the melt during the fuming period, and  $K$  is a constant.

Dividing Eq. (10) by Eq. (9) gives the change in fume with the  $O_2$  content of the gas bubble, Eq. (11)

$$\frac{d F}{d (N_{O_2})} = - \frac{K N_{N_2}}{K_g Pt N_{O_2}} \quad (11)$$

Once the  $O_2$  level in the bubble falls to the level where the Na evolved is not oxidized, fume generation essentially stops. Equation (11) can then be integrated between the following boundary conditions.

- 1) For initial moles of O<sub>2</sub> in bubble (N<sub>O<sub>2</sub>I</sub>), fume generation (F) = 0. This boundary condition is simply that no fume is generated until the gas is introduced into the melt and the oxidation process begins.
- 2) For O<sub>2</sub> remaining in bubble when fuming stops (N<sub>O<sub>2</sub>F</sub>), fume generated = measured fume (F<sub>M</sub>). This condition is that once the O<sub>2</sub> concentration in the bubble falls below that required to rapidly oxidize the Na evolving from melt, fuming stops and the fume present in the bubble is the measured fume F<sub>M</sub>.

$$\int_0^{F_M} dF = - \frac{K N_{N_2}}{kg Pt} \int_{N_{O_2I}}^{N_{O_2F}} \frac{dN_{O_2}}{N_{O_2}} \quad (12)$$

$$F_M = \frac{K N_{N_2}}{Kg Pt} [\ln (N_{O_2I}) - \ln (N_{O_2F})] \quad (13)$$

To test this model of fume generation, the fume generation rates were plotted vs. the ln of the initial O<sub>2</sub> flow rates, Figure (10), for the three different carrier gases in Table 7. From Eq. (13), this plot of the ln of the initial O<sub>2</sub> molar flow rates vs. the fume generation rate should yield a straight line.

(Figure 10 here)

As illustrated in Figure 10, Eq. (13) accurately describes the effect of O<sub>2</sub> on fume generation during sulfide oxidation with the purge introduced below the melt's surface. In Figure 10, fume generation is clearly a logarithmic function of the initial O<sub>2</sub> content of the purge.

The lower fume generation rate in He is due to O<sub>2</sub> having a higher diffusivity in He than it has in either Ar or N<sub>2</sub>. This higher diffusivity results in faster consumption of the O<sub>2</sub> and hence a shorter time for fume generation.

The penetration theory first proposed by Higbie (1935) predicts that the mass transfer coefficient should be proportional to the square root of the diffusivity, as given by Eq. (14).

$$K_A \propto D_A^{1/2} \quad (14)$$

Then from Eq. (13), the fume generated as the bubble passes through the melt should be inversely proportional to the square root of the interdiffusivity of  $O_2$  in the carrier gas.

To confirm this, the diffusivities for  $O_2$  in the three inert carrier gases were calculated using the Wilke and Lee (1955) modification of the equation by Hirschfelder, Bird and Spatz (1949).

Table 9 lists the calculated diffusivities of  $O_2$  in the three carrier gases used in this study, the predicted fuming rates relative to the  $N_2-O_2$  system, and the actual fuming rates relative to the  $N_2-O_2$  system. The actual relative fuming rates in this table are the averages of the relative fuming rates for different  $O_2$  levels. The predicted relative fuming rates are based on the change in the gas mass transfer coefficient resulting from changes in the diffusivities of  $O_2$  in the carrier gases. As shown in this table, the actual relative fuming rates are quite close to those predicted on the basis of changes in  $O_2$  diffusivities in the carrier gases.

(Table 9 here)

This mechanism for enhanced fuming under oxidizing conditions accurately explains the effects of the experimental variables on fume generation during sulfide oxidation. The major effects of the experimental variables on fume generation and their relationship to the proposed mechanism are summarized below.

(A) Fume generation during sulfide oxidation with the  $N_2-O_2$  gas system introduced above melt's surface.

1. Fume generation with a  $N_2-O_2$  gas was normally less than that with a pure  $N_2$ . This results from the sulfide oxidation rate being liquid side mass transfer limited in this mode of gas-melt contact. The melt at the gas-melt interface is oxidized and the vapor pressure of Na is low in this oxidized state.
2. Only at very low  $O_2$  partial pressures was the fume generation rate greater than that with a  $N_2$  atmosphere. This results when the low  $O_2$  partial pressures are not sufficient to oxidize the melt's surface. Sodium then vaporizes from the melt and is oxidized in the gas above the melt. This creates a Na sink and increases the rate of Na vaporization.

(B) Fume generation during sulfide oxidation with the  $N_2-O_2$  gas introduced below the melt's surface.

1. Sulfide oxidation in this mode of gas-melt contact produces large quantities of fume. This results from sulfide oxidation being gas-side mass transfer limited. The melt at the gas-melt interface has a relatively high Na vapor pressure. As soon as this Na evolves from the melt it is oxidized in the gas phase. This oxidation drastically lowers the partial pressure of the Na in the gas and increases the vaporization rate.

2. The rate of fuming is nearly proportional to the  $N_2$  purge rate. This results from the rate of oxygen consumption in the gas bubble being inversely proportional to the  $N_2$  flow rate, Eq. (9). Therefore, as the  $N_2$  purge rate increases, the time required for complete consumption of the  $O_2$  in the gas is also increased and more fume is generated.
3. The fume generation rate depends logarithmically on the initial  $O_2$  content of the gas. This results from the rate of consumption of  $O_2$  in the gas bubble being proportional to the  $O_2$  concentration. The rate of  $O_2$  consumption is then a logarithmic function. This logarithmic dependence of the fuming rate is predicted by Eq. (13).
4. The bubble size and hence surface area had no effect on the fume generation rate. This results from the rate of sulfide oxidation, Eq. (9), and the rate of fume generation, Eq. (10), both being directly proportional to the surface area. Since the surface area drops out when these equations are combined, Eq. (11), the surface area of the gas bubble does not affect the fume generation rate.
5. Fume generation during sulfide oxidation is not dependent on the  $Na_2SO_4$  and  $Na_2S$  content of the melt. This results from the very weak dependence of Na vapor pressure on the concentration of these compounds, Eq. (2).
6. Carrier gases with higher  $O_2$  interdiffusivities produce lower fume generation rates. This results from higher

interdiffusivities producing faster rates of O<sub>2</sub> consumption. Since the O<sub>2</sub> in the bubble is consumed faster, fuming lasts for a shorter period of time and less fume is produced.

## DISCUSSION

The experimental results of this study demonstrate that enhanced fume generation during Na<sub>2</sub>S oxidation results from the Na oxidation in the gas phase. Although fume generation was studied in rising gas bubbles, the mechanism for enhanced fume generation can occur anytime an oxidizing atmosphere contacts a reduced melt. All this mechanism requires is that there is enough mixing in the melt that the melt's surface is renewed faster than it is oxidized. This may occur anytime turbulent conditions exist. Therefore, this mechanism likely has a significant effect on the amount of fume generated in the kraft furnace.

Although the vapor pressure of Na in the melts used for this study is relatively low, the reduction in gas-side resistance to Na vaporization resulting from gas phase Na oxidation can result in significant quantities of Na based fume. The maximum rate of Na vaporization under these conditions is the rate in vacuo and is given by the Langmuir equation.

$$J_{\text{Max}} = \frac{P_{\text{Na}}}{\sqrt{2\pi RT M_{\text{Na}}}} \quad (15)$$

Here,  $J_{\text{max}}$  is the maximum vaporization rate;  $P_{\text{Na}}$  is the vapor pressure of Na; and  $M_{\text{Na}}$  is Na's molecular weight.

From estimates of bubble diameter, terminal velocity and melt level, the melt-gas interfacial area present during the fuming experiments is in the

range of a  $100 \text{ cm}^2$ . With this surface area, the Langmuir equation predicts that the minimum Na vapor pressure necessary to produce the observed fuming rate is  $10^{-7}$  atm at  $1200^\circ\text{K}$ . From the free energy, the equilibrium Na vapor pressure for reaction (1) is estimated to be approximately  $2 \times 10^{-4}$  atm. The vapor pressure of Na is then three orders of magnitude greater than that required to produce the observed fuming rate.

The actual fuming rate is less than the maximum for 3 reasons: 1) fume is generated only as long as  $\text{O}_2$  is present in the gas bubble, 2) all Na gas phase oxidation may not occur at the gas-melt interface and 3) the partial oxidation of the melt may produce a Na vapor pressure less than that predicted from the equilibrium calculation. This analysis shows that the Na vapor pressure in the melt is more than sufficient to produce the observed fuming rate.

#### CONCLUSIONS

The major conclusions reached in this study are summarized below:

1. Fume production is a dynamic process, dependent on mass transfer processes and chemical reactions. This implies that fume in a kraft recovery furnace is more than an equilibrium phenomenon, and that fume production is a potentially manipulatable process.
2. Sodium vaporization can be significant during sulfide oxidation in a  $\text{Na}_2\text{CO}_3\text{-Na}_2\text{S}$  melt and can result in large quantities of  $\text{Na}_2\text{CO}_3$  fume. This was an unexpected result, since Na is a reduced species and was previously not thought to be present during an oxidative process.
3. Fume produced during sulfide oxidation results from the oxidation of Na vapor in the gas phase. This oxidation of Na produces a

Na sink in the gas phase, reducing the partial pressure of Na and the mass transfer resistance to vaporization. This vapor sink significantly increases the rate of Na vaporization.

#### LITERATURE CITED

1. Bauer, T. W.; Dorland, R. M., Can. J. Techn. 32, 91 (1954).
2. Cameron, J. H.; Clay, D. T.; and Grace, T. M. 1985 International Chemical Recovery Conference 11-2, 435; New Orleans, LA.
3. Clay, D. T.; Grace, T. M.; Kapheim, R. J. AIChE Symposium Series 239, 80, 99 (1984).
4. Hirschfelder, J. O.; Bird, R. B.; Spatz, E. L., Trans. Am. Soc. Mech. Engrs. 71, 921 (1949).
5. Turkdogan, E. T.; Grieveson, P.; Darken, L. S., J. Phys. Chem. 67, 1647 (1963).
6. Turkdogan, E. T. Physical chemistry of high temperature technology. Academic Press, New York, 1980.
7. Turkdogan, E. T.; Grieveson, P.; Darken, L. S. Proc. Natl. Hearth Steel Con. 470 (1982).
8. Warnqvist, B., Svensk Papperstid. 76(12), 463-6 (1973).
9. Wilke, C. R.; Lee, C. Y., Ind. Eng. Chem. 47, 1253 (1955).

Table 1. Typical experimental fume generation results with purge introduced below the melt's surface

Run 38

Initial Melt Composition

Na<sub>2</sub>CO<sub>3</sub> = 0.77 mole

Na<sub>2</sub>S = 0.03 mole

Purge = 1 L/min at 2.1% O<sub>2</sub>

Temperature = 927°C

Time, s	<u>Calculated Composition</u>		Fume Generation Rate, g/min	<u>Fume Concentration</u>
	Na <sub>2</sub> SO <sub>4</sub> , mole/L	Na <sub>2</sub> S, mole/L		Moles Na <sub>2</sub> CO <sub>3</sub> Mole N <sub>2</sub>
755	0.136	0.549	0.0099	0.00214
1280	0.231	0.455	0.0104	0.00224
1760	0.318	0.368	0.0106	0.00288
2240	0.405	0.281	0.0104	0.00224
2721	0.492	0.195	0.0099	0.00214
3114	0.563	0.124	0.0088	0.00190
3639	0.656	0.029	0.0005	0.00011

Table 2. Effect of sulfate level on fume generation rate.

Purge Rate = 1.0 L/min at 2.1% O <sub>2</sub> , and	Temperature = 982°C
Run 39	Run 43
Na <sub>2</sub> CO <sub>3</sub> = 0.77 mole	Na <sub>2</sub> CO <sub>3</sub> = 0.57 mole
Na <sub>2</sub> S = 0.03 mole	Na <sub>2</sub> S = 0.03 mole
Na <sub>2</sub> SO <sub>4</sub> = 0.00 mole	Na <sub>2</sub> SO <sub>4</sub> = 0.30 mole

Time, min	Fume Generation Rate, g/min	Fume Generation Rate, g/min
5	0.0157	0.0125
10	0.0159	0.0127
15	0.0161	0.0121
20	0.0145	0.0149
25	0.0158	0.0103
30		0.0103
35	Std. Dev.	Std. Dev.
Ave.	0.0158 ± 0.0006	0.0130 ± 0.0019

Table 3. Effect of sulfide level on fume generation rate.

Conditions: Temperature = 954°C

N<sub>2</sub> Flow Rate = 1.0 L/Min

O<sub>2</sub> Flow Rate = 0.021 L/min

Na <sub>2</sub> CO <sub>3</sub> mole	Na <sub>2</sub> S mole	Sulfidity, %	Fume Generation Rate g/min ± Std. Dev.
0.77	0.03	3.7	0.0142 ± 0.001
0.60	0.20	25.0	0.0136 ± 0.001
0.55	0.25	31.0	0.0144 ± 0.001

Table 4. Effect of oxygen level in the purge on fume generation rate.

Temperature = 927°C

Run	N <sub>2</sub> L/min	O <sub>2</sub> L/min	Fume Generation Rate, g/min
45	1.02	0.0105	0.00892
46	1.02	0.021	0.0105
47	1.02	0.042	0.0121
48	1.01	0.063	0.0145
49	1.02	0.084	0.0146

Table 5. Effect of purge rate on fume generation.

Initial Melt Conditions:  $\text{Na}_2\text{CO}_3 = 0.77$  mole  
 $\text{Na}_2\text{S} = 0.03$  mole  
 Temperature =  $927^\circ\text{C}$

Run	$\text{N}_2$ , L/min	Air, L/min	Total $\text{N}_2$ , L/min	Fume Generation Rate $\pm$ Std. Dev., g/min
50	0.04	0.1	0.48	$0.00680 \pm 0.00032$
51	0.6	0.1	0.68	$0.00850 \pm 0.00076$
52	0.8	0.1	0.88	$0.01004 \pm 0.00042$
38	0.9	0.1	0.98	$0.01024 \pm 0.00032$
53	1.06	0.1	1.14	$0.01204 \pm 0.00042$
54	1.23	0.1	1.31	$0.01474 \pm 0.00198$

Table 6. Effect of two purge tubes on fume generation rate.

Run No.	Temp., °C	N <sub>2</sub> Flow Rate, L/min	O <sub>2</sub> Flow Rate, L/min	Fuming Rate, g/min ± Std. Dev.	Fuming Rate with Single Purge Tube, g/min
127	953	1.03	0.020	0.0129 ± 0.001	0.0126
128	957	1.03	0.0426	0.0163 ± 0.001	0.0156
129	957	1.01	0.0634	0.0156 ± 0.001	0.0172

Table 7. Effect of carrier gas on fume generation.

Fume Generation Rates Using N<sub>2</sub>, Ar, and He

Conditions: N<sub>2</sub>, Ar, He = 1.0 L/min  
 O<sub>2</sub> = 0.01 to 0.20 L/min  
 Temperature = 955°C

Gas System	O <sub>2</sub> Purge Rate, L/min					
	0.01	0.03	0.05	0.10	0.15	0.20
	Fume Generation Rate, g/min					
N <sub>2</sub> -O <sub>2</sub>	0.0078	0.0128	0.0156	0.0184	0.00232	0.0210
Ar-O <sub>2</sub>	0.0086	0.0126	0.0139	0.0168	0.0182	0.0192
He-O <sub>2</sub>	0.0053	0.0076	0.0083	0.0114	0.0133	0.0142

Table 8. Effect of purge tube location on fume generation during sulfide oxidation.

Initial Conditions

Na<sub>2</sub>CO<sub>3</sub> = 0.77 mole  
 Na<sub>2</sub>S = 0.03 mole  
 Temperature = 955°C

Purge Introduced Below Melt's Surface		Purge Introduced Above Melt's Surface	
Oxidation Rate, mole O <sub>2</sub> consumed/min x 10 <sup>4</sup>	Fume Rate, g/min	Oxidation Rate, mole O <sub>2</sub> consumed/min x 10 <sup>4</sup>	Fume Rate, g/min
9.38	0.0106	0.84	0.00146
9.46	0.0134	3.88	0.00100
		7.80	0.00115
		12.00	0.00079
		17.70	0.00044

Table 9. Effect of gas diffusivity of fume generation.

Gas System	Diffusivity ± Av. Error, cm <sup>2</sup> /s	Predicted Relative to N <sub>2</sub> -O <sub>2</sub> Fuming Rates, g/min	Actual Relative to N <sub>2</sub> -O <sub>2</sub> Fuming Rates ± 1 Std. Dev., g/min
N <sub>2</sub> -O <sub>2</sub>	2.44 ± 0.1	1.0	1.0
Ar-O <sub>2</sub>	2.38 ± 0.1	1.01	0.93 ± 0.10
He-O <sub>2</sub>	8.08 ± 0.3	0.55	0.58 ± 0.07

### Oxidation Enhanced Metal Vaporization

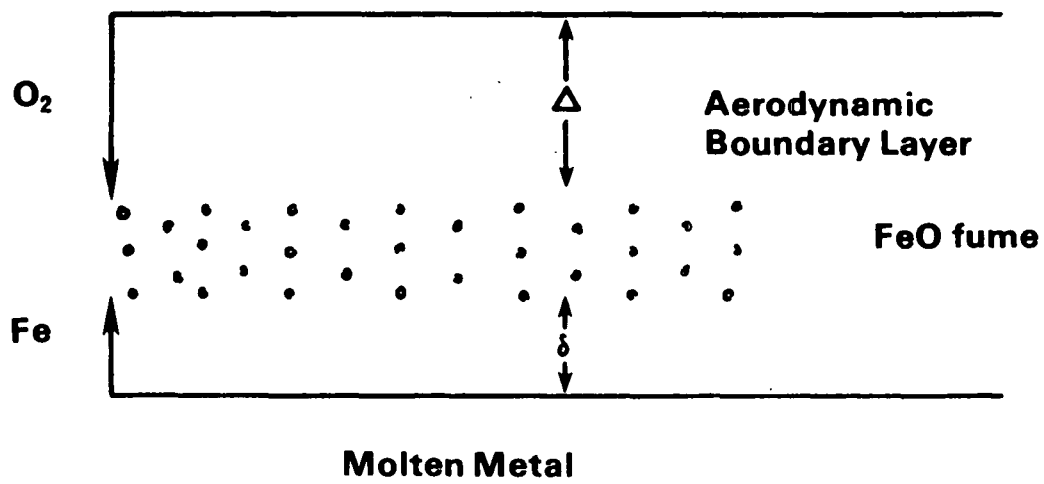


Figure 1. Gas phase oxidation enhanced vaporization.

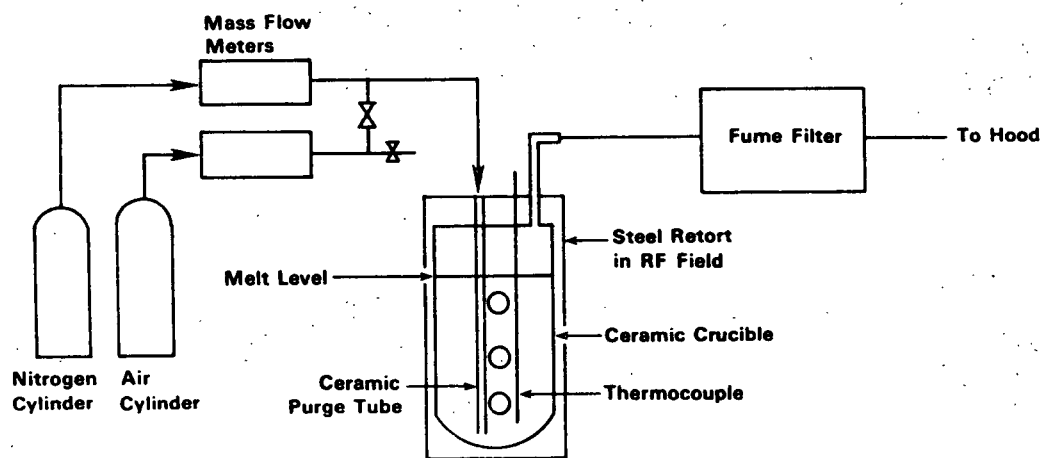


Figure 2. Experimental system.

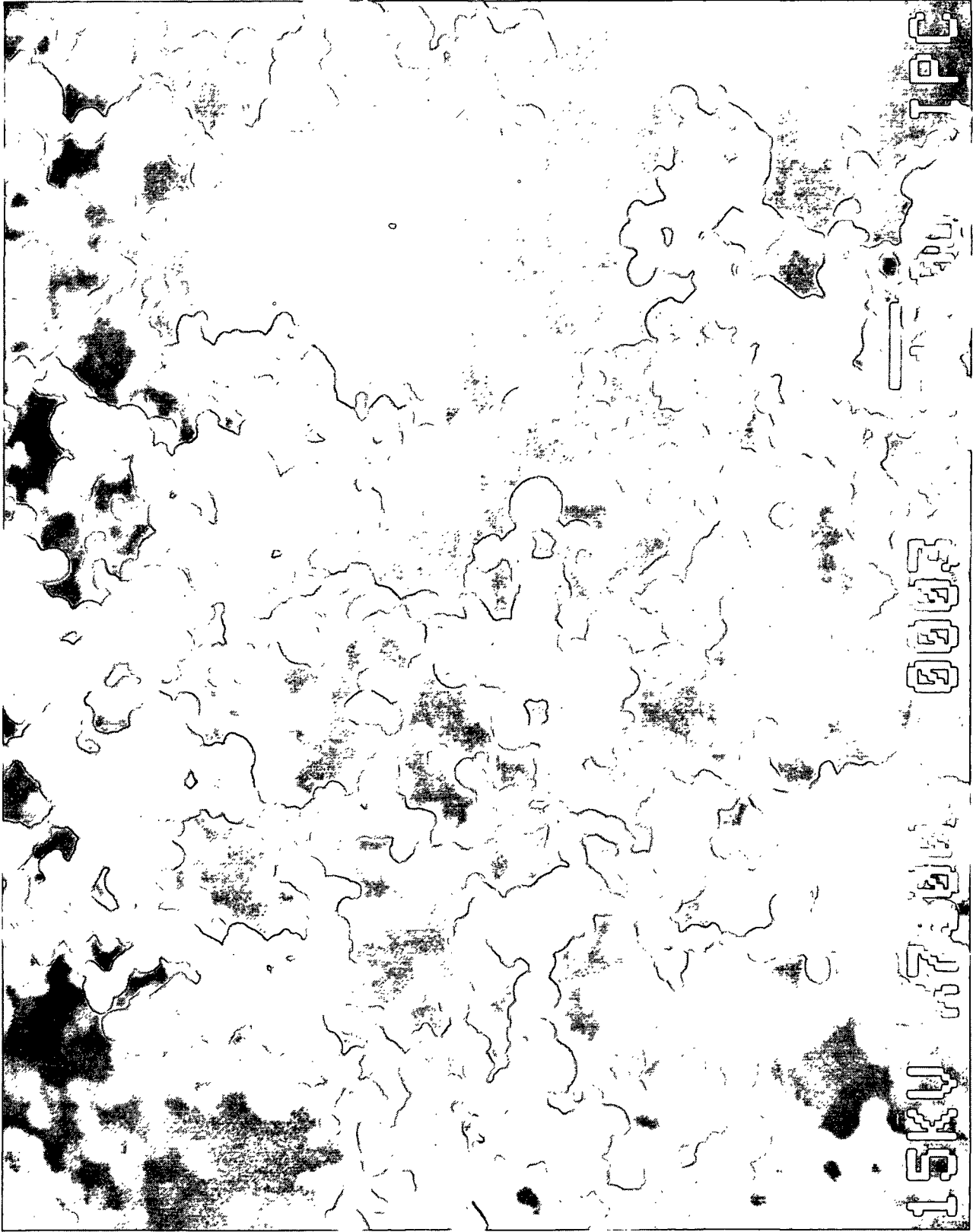


Figure 3. Fume particles collected during sulfide oxidation.

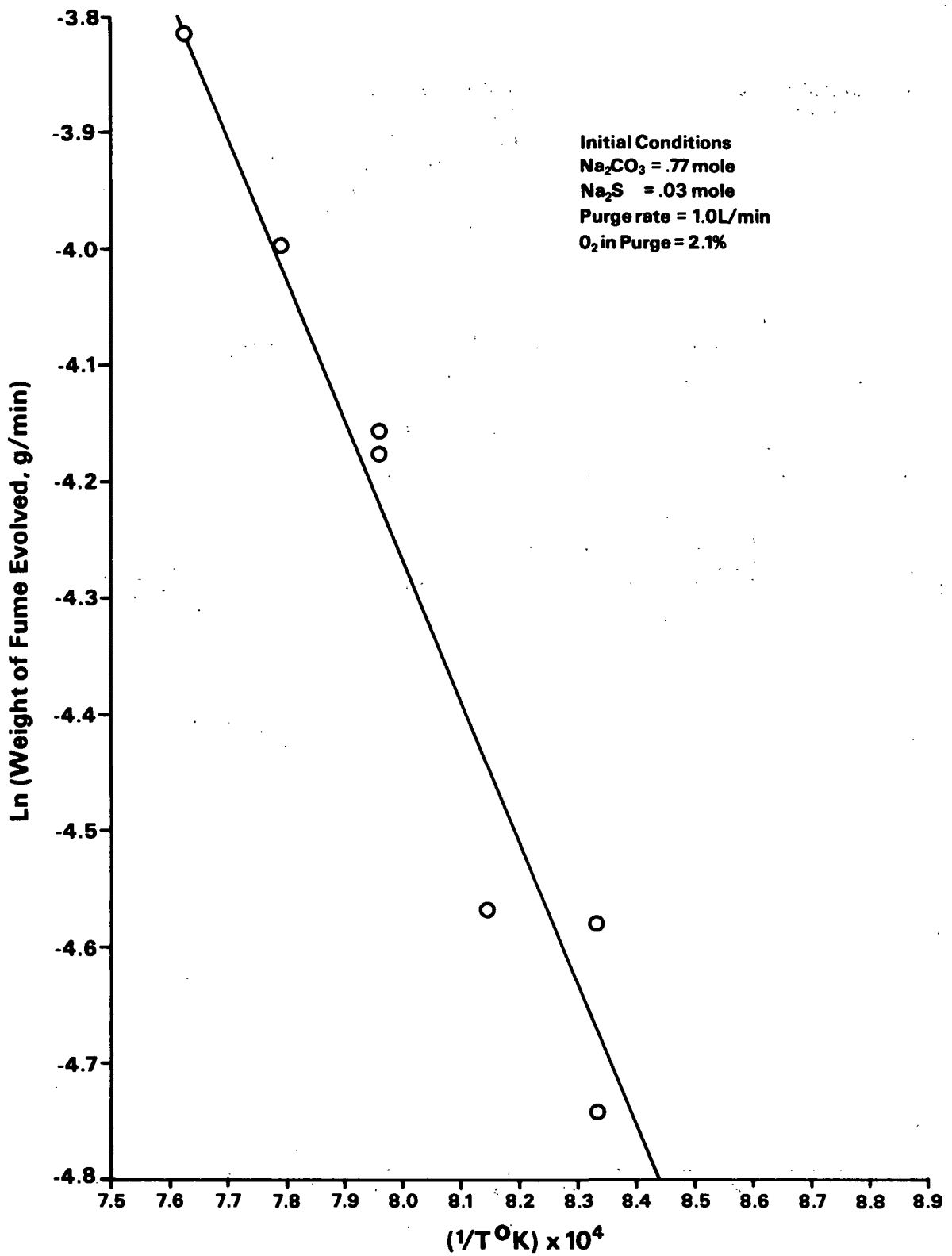


Figure 4. Effect of temperature on fume generation.

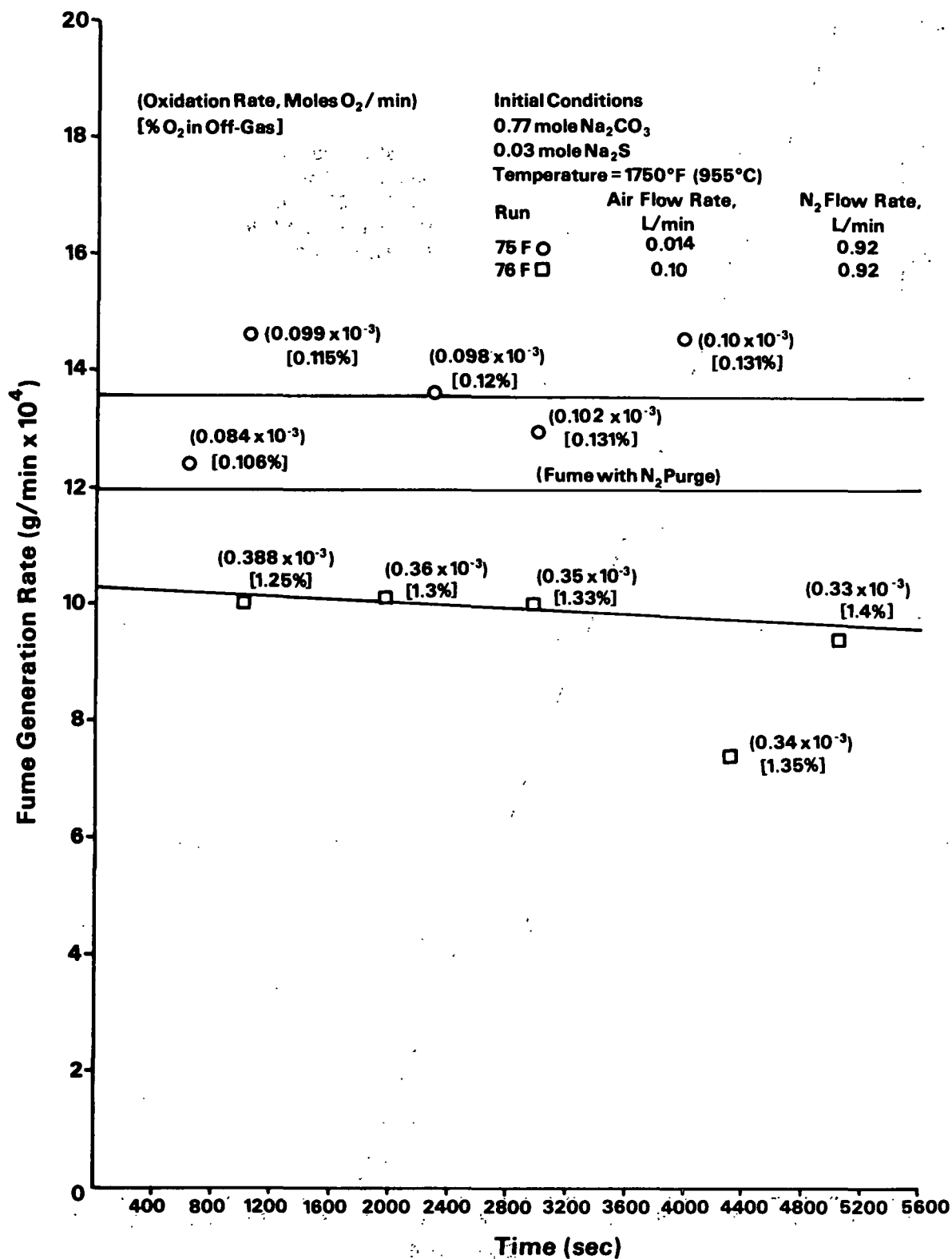


Figure 5. Effect of oxygen on fume generation with purge introduced above melt at low oxygen levels.

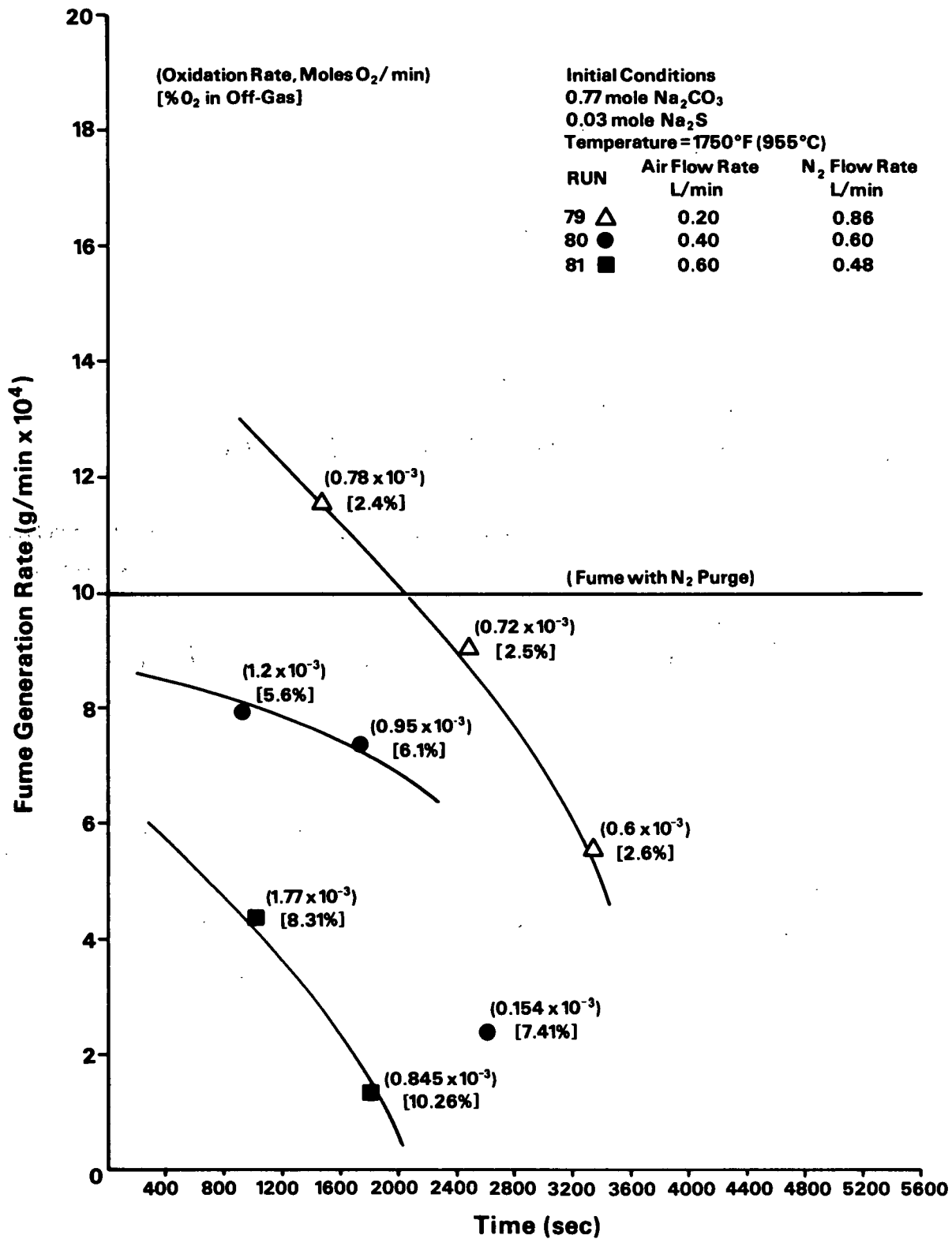


Figure 6. Effect of oxygen on fume generation with purge introduced above melt at high oxygen levels.

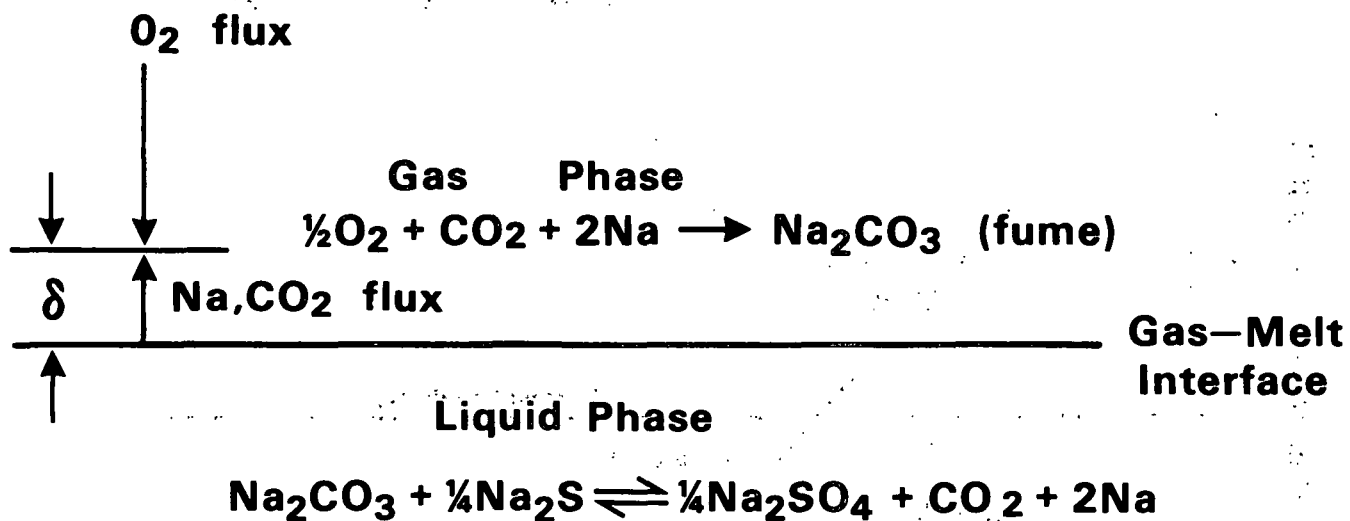


Figure 7. Fume generation under oxidizing conditions.

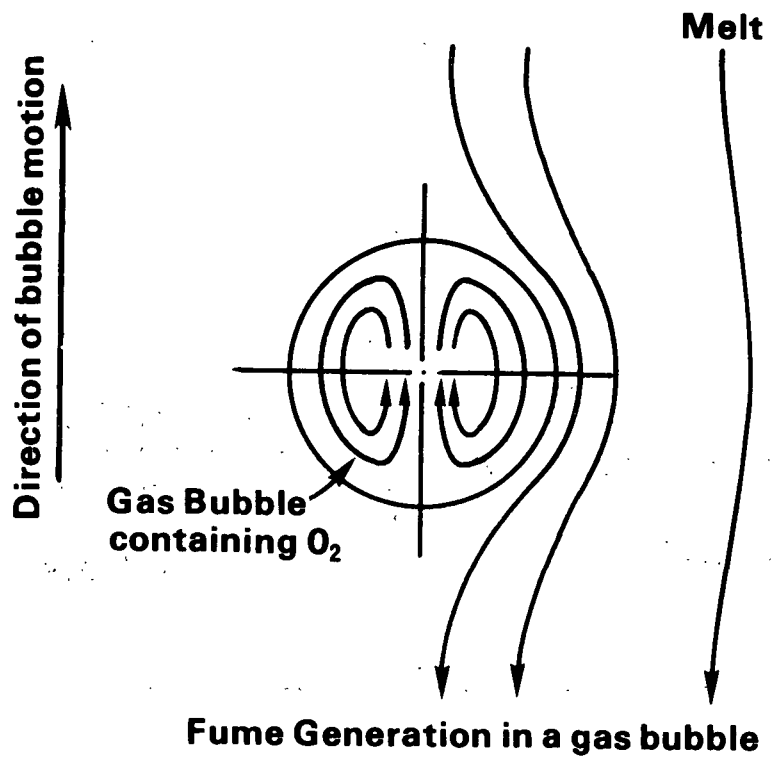


Figure 8. Fume generation in a rising gas bubble.

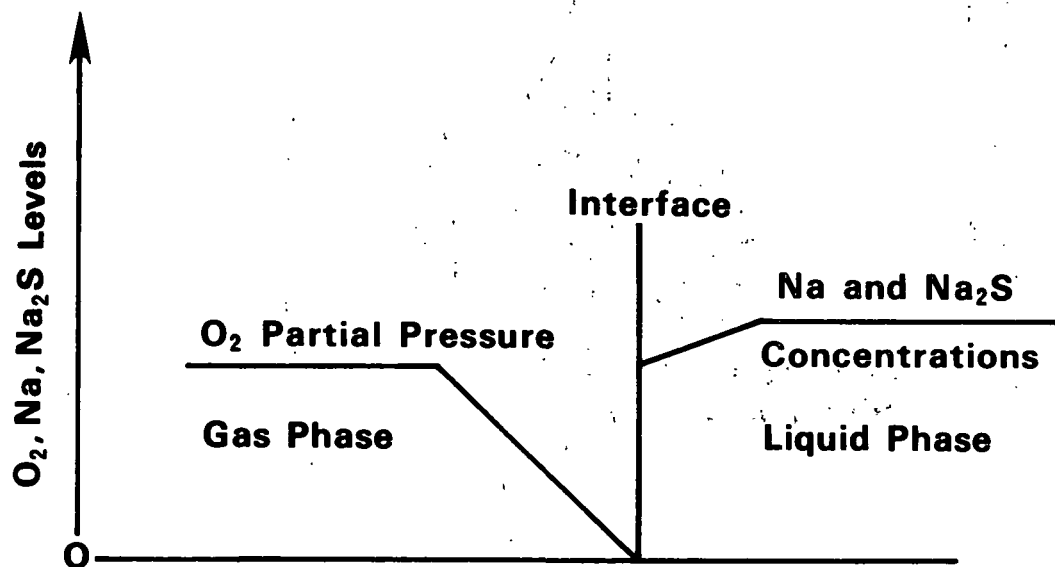


Figure 9. Relative levels of O<sub>2</sub>, Na, and Na<sub>2</sub>S at bubble interface during sulfide oxidation.

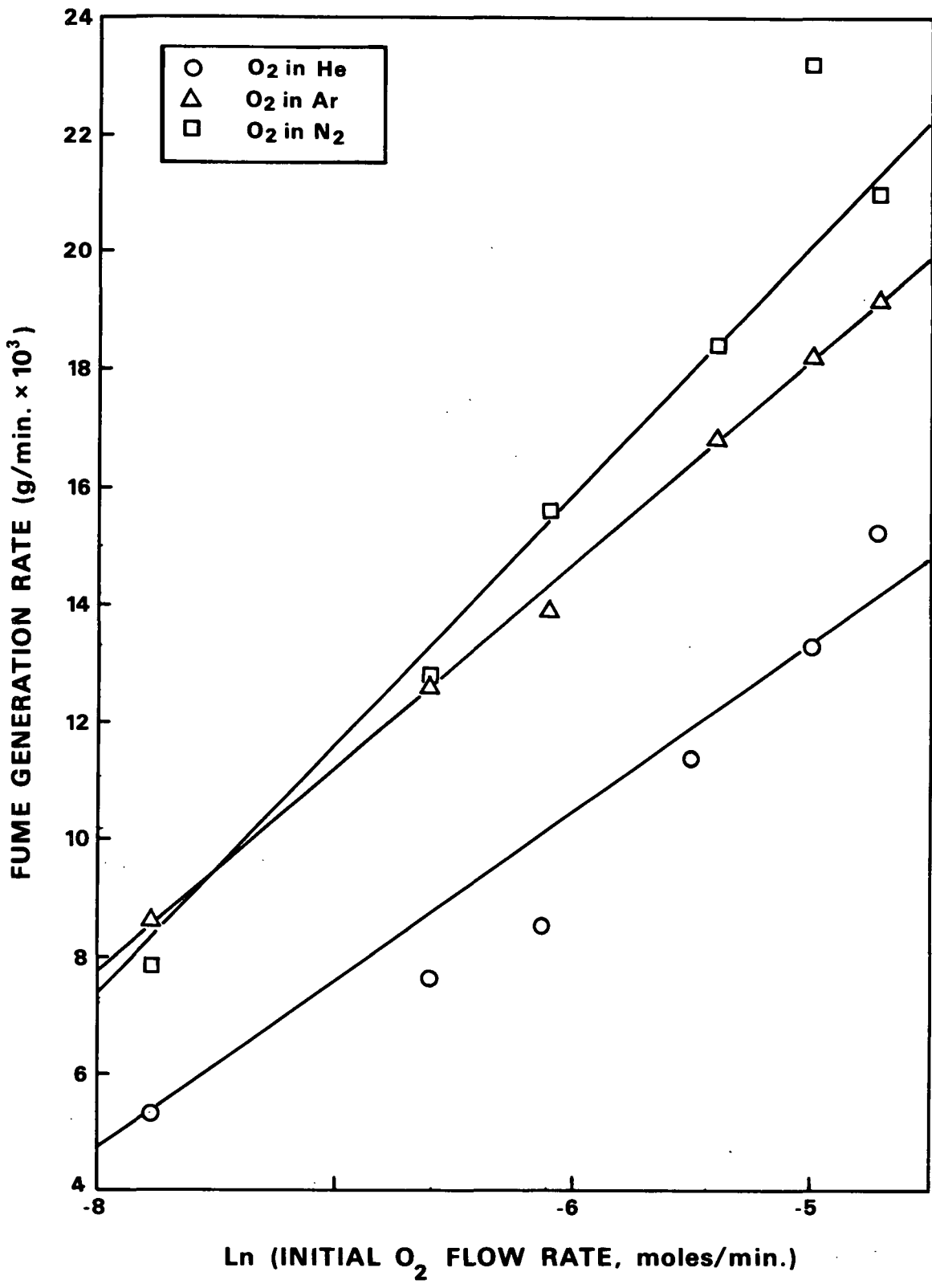


Figure 10. Effect of O<sub>2</sub> on fume generation in N<sub>2</sub>, Ar, and He.